ELSEVIER

Journal of Organometallic Chemistry 525 (1996) 159–166

Journal of Organometallic Chemistry

Steric effects along ligands in bis(trimethylsilyl)cyclopentadienyl complexes of ruthenium: analysis by radial profiles

Jeremy M. Smith, Stephen C. Pelly, Neil J. Coville *

Centre for Applied Chemistry and Chemical Technology, Department of Chemistry, University of the Witwatersrand, Johannesburg, Private Bag 3, PO Wits 2050, South Africa

Received 18 March 1996; revised 9 May 1996

Abstract

The new complexes $[(\eta^5\text{-}C_5H_3(SiMe_3)_2)Ru(CO)(L)I]$ (L = ^{t}BuNC, PMe_3, PPh_2Et, PPh_3, $P(OMe)_3$, $P(O^iPr)_3$, $P(OPh)_3$, and $P(O\text{-}o\text{-}tol)_3$ were prepared from the reaction between $[(\eta^5\text{-}C_5H_3(SiMe_3)_2)Ru(CO)_2I]$ and L in the presence of $[(\eta^5\text{-}C_5H_3(SiMe_3)_2)Ru(CO)_2]_2$ as catalyst. Analysis of the complexes with L = PMe_3, PPh_3 and $P(O\text{-}o\text{-}tol)_3$ by the nOe technique revealed restricted rotation of the cyclopentadienyl ligand with the ligand rotation decreasing with increasing size of L. No free rotation of the cyclopentadienyl ring in the analogous $[(\eta^5\text{-}C_5H_3(SiMe_3)_2)Fe(CO)(L)I]$ complexes was observed. Regression analysis of NMR spectral parameters for the various cyclopentadienyl ring protons, as well as solid angle radial profiles, cone angle radial profiles and solid angle of overlap (Γ) radial profiles identified that the differences between the ruthenium and iron complexes were related to the steric interaction between the hydrogen atoms of the trimethylsilyl ring substituents and L.

Keywords: Cyclopentadienyl; Ruthenium; Steric effect; Solid angle; Cone angle; Radial profile

1. Introduction

In previous studies we have explored the intramolecular steric interactions in $[(\eta^5\text{-}C_5H_4R)M(CO)(L)I]$ (M = Fe, Ru; R = Me, ^{t}Bu, $SiMe_3$, COOMe, I, $CHPh_2$, ^{i}Pr, Ph, CPh_3; L = phosphine, phosphite, isonitrile) complexes [1–3] between the cyclopentadienyl ring and the ligand set (CO, L, I) by NMR spectroscopy. Assignment of a size parameter to the cyclopentadienyl ring and L group (e.g. Tolman cone angle θ [4], solid angle Ω_s [5]) has permitted a correlation between the NMR spectral parameters of these complexes and the steric properties associated with the cyclopentadienyl ring and L. More recently, a study of a bis(trimethylsilyl)cyclopentadienyl iron system, $[(\eta^5\text{-}C_5H_3(SiMe_3)_2)Fe(CO)(L)I]$, suggested that substantial steric interaction occurred between the $SiMe_3$ group and L [3], which restricted free rotation of the cyclopentadienyl ring relative to the ligand set (CO, L, I).

In this publication we report the synthesis, characterisation, and analysis of a series of $[(\eta^5\text{-}C_5H_3(SiMe_3)_2)Ru(CO)(L)I]$ complexes in order to establish the influence of the metal atom on the ring rotational behaviour. In particular, we wished to determine and assess the nature of the interaction between the ring and the ligand set (CO, L, I). This is made possible by our investigations into steric measurement techniques which have allowed us to develop theoretical tools for (i) quantifying the possible steric congestion within a complex [6] and (ii) establishing factors that influence the variation in steric requirements of a ligand in a complex [7].

Herein we have applied various steric measures, i.e. solid angle radial profiles (SARP), cone angle radial profiles (CARP) [8] and solid angle of overlap profiles (Γ) to qualitatively and quantitatively evaluate steric effects in the new complexes. These techniques have also allowed us to assess the effect of a change in metal atom (Fe for Ru) on the steric measures.

2. Results and discussion

2.1. Synthesis

The reaction of $[Ru_3(CO)_{12}]$ and bis(trimethylsilyl)cyclopentadiene in heptane, followed by addition

* Corresponding author.

PII S0022-328X(96)06449-2

Table 1
^{1}H NMR and IR data for [(η^5-$C_5H_3(SiMe_3)_2$)Ru(CO)(L)I] complexes [a]

L	*H2*	*H4*	*H5*	$Si(CH_3)_3$		L	J_{P-H}	ν_{CO} (cm^{-1})
CO	5.46	4.78		0.142				2040, 1994
^{t}BuNC	5.42	4.98	4.92	0.281		0.995 (CH_3)		1946
$P(OMe)_3$ [b]	5.47	5.03	4.79	0.368	0.268	3.40, 3.34 (CH_3)	2.4	1978
PMe_3 [c]	5.33	4.55	4.47	0.277	0.268	1.32, 1.27 (CH_3)		1946
$P(OPh)_3$	5.67	4.81	4.05	0.387	0.206	7.36–7.29 (*o*-Ph), 7.01–6.79 (*m*, *p*-Ph)	3.4	1978
$P(O^iPr)_3$ [d]	5.35	5.13	4.95	0.444	0.273	4.90–4.79 (CH), 1.23–1.18 (CH_3)		1974
$PMePh_2$ [e]	5.52	4.64	4.32	0.349	0.329	7.70–7.58 (*o*-Ph), 7.20–7.11 (*m*, *p*-Ph), 2.36, 2.32 (CH_3)		1948
$PEtPh_2$ [f]	5.28	4.32	4.12	0.254	0.200	7.64–7.54 (*o*-Ph), 7.11–7.00 (*m*, *p*-Ph), 2.62, 2.89 (CH_2), 0.847–0.688 (CH_3)		1944
$P(O\text{-}o\text{-}tol)_3$	5.68	5.08	3.96	0.378	0.203	7.54–7.49 (*o*-Ph), 6.87–6.71 (*m*, *o*-Ph), 2.35 (CH_3)	2.2	1982
PPh_3	5.44	4.14	4.01	0.316	0.283	7.81–7.69 (*o*-Ph), 7.08–6.96 (*m*, *p*-Ph)		1946

[a] Recorded in C_6D_6 at 22 °C, δ in ppm relative to TMS.
[b] J_{C-H} = 11 Hz. [c] J_{C-H} = 10 Hz. [d] J_{C-H} = 4 Hz. [e] J_{C-H} = 9 Hz. [f] J_{C-H} = 17 Hz.

of methyl iodide, gave [(η^5-$C_5H_3(SiMe_3)_2$)$Ru(CO)_2I$] in reasonable yield [9]. Small quantities of [(η^5-$C_5H_3(SiMe_3)_2$)$Ru(CO)_2$]$_2$ were also obtained from the reaction. Both new products were characterised by IR and NMR spectroscopy (Tables 1 and 2). Substitution of one of the carbonyl ligands by PPh_3 was carried out to establish the best reaction conditions for producing [(η^5-$C_5H_3(SiMe_3)_2$)Ru(CO)(L)I] (L = PPh_3). In refluxing benzene as solvent, the reaction was found to be complete within 2 h. This reaction time was reduced to 30 min by addition of ca. 10% (w/w) of the dimer complex [(η^5-$C_5H_3(SiMe_3)_2$)$Ru(CO)_2$]$_2$ [10].

Carbonyl substitution by a range of other phosphine and phosphite ligands generally occurred in excellent yield in the presence of the dimer catalyst under the conditions established for the PPh_3 ligand. All complexes were characterised by IR, ^{1}H and ^{13}C NMR spectroscopy, and by elemental analysis for the solid products. Spectral data are listed in Tables 1 and 2. Reaction with the small tertiarybutylisocyanide ligand (θ = 68°, Ω_s = 0.085) was found to give both the mono- and disubstituted products [(η^5-$C_5H_3(SiMe_3)_2$)-$Ru(CO)_n(^tBuNC)_{2-n}I$] (n = 0, 1), while attempted substitution by the large ligands PBz_3 (θ = 165°, Ω_s = 0.428) and P(*o*-tol)$_3$ (θ = 194°, Ω_s = 0.366) did not yield any new products.

2.2. NMR spectrocopic study

All ^{1}H and ^{13}C NMR spectra of the new complexes showed the predicted number of signals in the correct intensity ratios. Proton NMR ring resonances (see Fig. 1 for numbering scheme) were assigned on the basis of visual inspection [1] and confirmed by nOe experiments. Separation of the three ring proton resonances was smaller than observed for the analogous iron complexes [3]. The H–H and P–H ring coupling constants were, in most cases, too small to be measured, as has been found with similar ruthenium complexes [2]. Carbon-13 NMR ring resonances were assigned on the same basis as those in the analogous [(η^5-$C_5H_3(SiMe_3)_2$)Fe(CO)(L)I] system [3], where both carbons C2 and C3 were found to be coupled to phospho-

Table 2
^{13}C NMR data for [(η^5-$C_5H_3(SiMe_3)_2$)Ru(CO)(L)I] complexes [a]

L	*C1*	*C2*	*C3*	*C4*	*C5*	CO	$Si(CH_3)_3$		L [b]	J_{P-C2}	J_{P-C3}
^{t}BuNC	89	104.0	89.24	92.18	93.44	201.7	0.428		30.38 (CH_3)		
$P(OMe)_3$ [c]		100.8	92.82	90.12	95.62	203.3	0.567	0.160	52.08 (CH_3)	4.39	4.16
PMe_3 [d]		100.5		85.89	92.73		0.693	0.291	22.49 (CH_3)	5.41	
$P(OPh)_3$	94.81	106.5	93.35	86.20	93.86	201.7	0.635	0.014		7.21	9.21
$P(O^iPr)_3$ [e]	89.10	100.1	99.48	91.58	93.29	204.0	0.913	0.293	71.18 (CH), 24.13 (CH_3)	6.85	5.88
$PMePh_2$ [f]	100.2	97.78	93.98	85.00	96.70	204.5	0.569	−0.054	22.11 (CH_3)	7.08	4.56
$PEtPh_2$ [g]	103.7	93.91	95.03	84.25	98.98	205.1	0.555	−0.182	27.79 (CH_2), 8.87 (CH_3)	7.69	3.62
$P(O\text{-}o\text{-}tol)_3$	95.86	105.5	95.38	83.31	94.98	203.0	0.625	−0.124	17.43 (CH_3)	9.50	10.11
PPh_3	100.8	97.62		84.90	98.41		0.549	0.036		7.28	

[a] Recorded in C_6D_6 at 22 °C, δ in ppm relative to TMS.
[b] Aromatic resonances not listed.
[c] J_{C-P} = 29.6 Hz. [d] J_{C-P} = 33.8 Hz. [e] J_{C-P} = 6.0 Hz. [f] J_{C-P} = 34.7 Hz. [g] J_{CH_3-P} = 4.4 Hz, J_{CH_2-P} = 31.9 Hz.

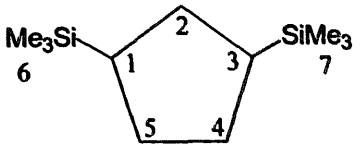

Fig. 1. Ring numbering scheme.

rus. However, not all quaternary ring carbon resonances could be identified.

2.2.1. NOe conformational analysis

As in previous studies [1–3], we have used the nOe technique to determine the solution conformers of the new complexes. In particular, nOe studies of $[(\eta^5\text{-}C_5H_3(SiMe_3)_2)Ru(CO)(L)I]$ with $L = PPh_3$, PMe_3 and $P(O\text{-}o\text{-}tol)_3$ were performed. Some nOe spectra for $[(\eta^5\text{-}C_5H_3(SiMe_3)_2)Ru(CO)(PPh_3)I]$ are shown in Fig. 2. Irradiation of the *ortho* phenyl proton resonance of PPh_3 (Fig. 2(b)) results in the growth of the resonances corresponding to the cyclopentadienyl ring protons in positions 2, 4 and 5. Preferential growth of the protons in positions 4 and 5 is to be noted, suggesting that L resides on average closer to protons 4 and 5 than to proton 2. Unequal growth of the resonances corresponding to the trimethylsilyl protons is also observed. This suggests that the preferred room temperature solution conformation of the complex has the phosphine ligand occupying a position closer to ring proton H4 and trimethylsilyl protons H7 (Fig. 3), but that cyclopentadienyl ring rotation through 360° relative to the ligand set still occurs. This is in contrast to the analogous iron system, where restricted ring rotation was detected [3] (see below). Irradiation of the *meta/para* phenyl ring proton resonances (Fig. 2(c)) gives a similar result. Irradiation of the resonances corresponding to protons H2, H4 and H5 and the trimethylsilyl proton resonances (not shown) confirm the results.

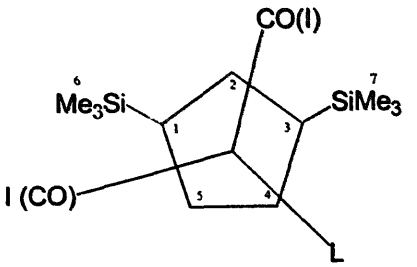

Fig. 3. Preferred solution conformation of $[(\eta^5\text{-}C_5H_3(SiMe_3)_2)\text{-}Ru(CO)(L)I]$.

An nOe study of $[(\eta^5\text{-}C_5H_3(SiMe_3)_2)Ru(CO)(PMe_3)I]$ (Fig. 4) produced similar results. Once again, the preferred conformation was found to be that shown in Fig. 3. When $[(\eta^5\text{-}C_5H_3(SiMe_3)_2)Ru(CO)(P(O\text{-}o\text{-}tol)_3)I]$ was studied by the nOe technique, very small growth of the H2 resonance occurred when the *ortho* phenyl protons were irradiated (Fig. 5(b)). In

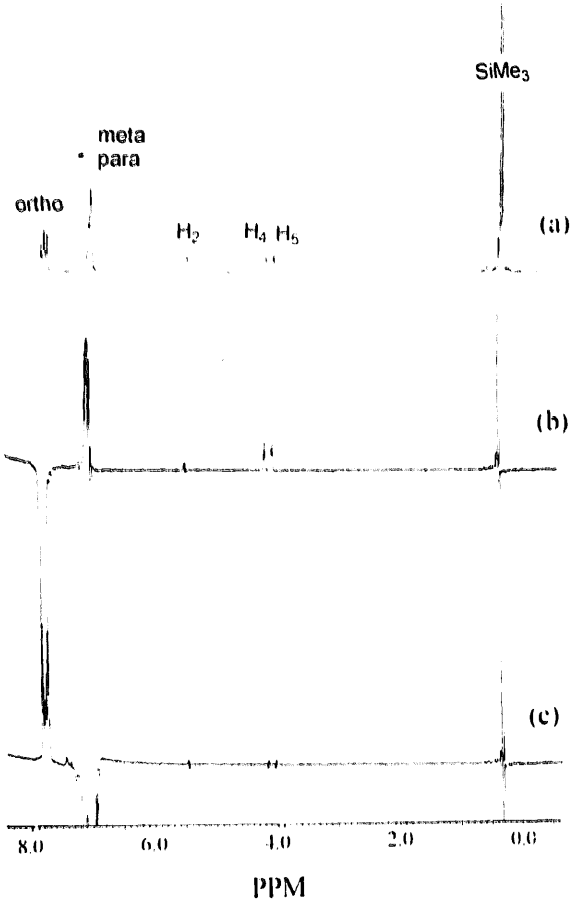

Fig. 2. Selected nOe difference spectra of $[(\eta^5\text{-}C_5H_3(SiMe_3)_2)\text{-}Ru(CO)(PPh_3)I]$. (a) Reference spectrum (no irradiation). (b) Irradiation of PPh_3 *ortho* ring protons. (c) Irradiation of PPh_3 *meta* and *para* ring protons.

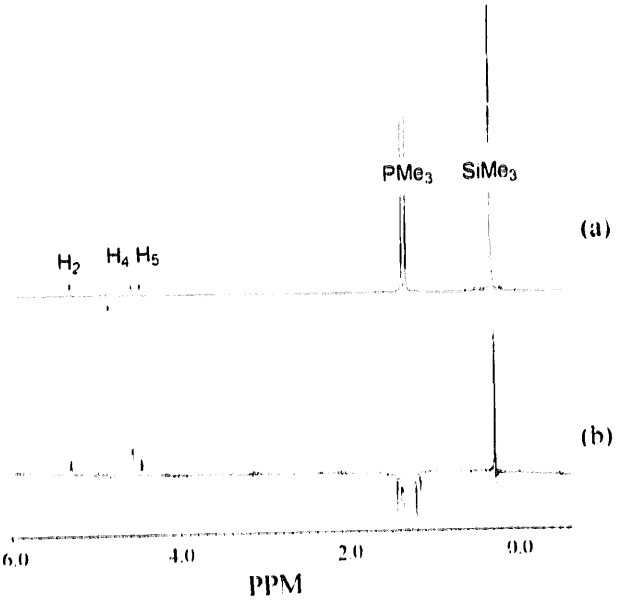

Fig. 4. Selected nOe difference spectra of $[(\eta^5\text{-}C_5H_3(SiMe_3)_2)Ru(CO)(PMe_3)I]$. (a) Reference spectrum (no irradiation). (b) Irradiation of PMe_3 protons.

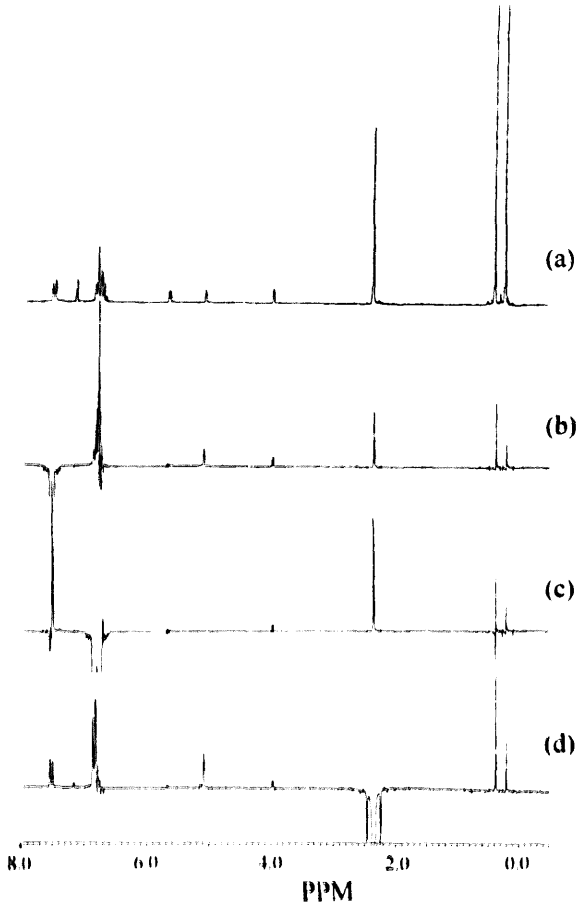

Fig. 5. Selected nOe difference spectra of $[(\eta^5\text{-}C_5H_3(SiMe_3)_2)Ru(CO)P(O\text{-}o\text{-}tol_3))I]$. (a) Reference spectrum (no irradiation). (b) Irradiation of P(O-*o*-tol)$_3$ *ortho* ring protons. (c) Irradiation of P(O-*o*-tol)$_3$ *meta* and *para* ring protons. (d) Irradiation of P(O-*o*-tol)$_3$ *ortho* methyl protons.

addition, when the *meta/para* protons of the P(O-*o*-tol)$_3$ ligand are irradiated (Fig. 5(c)), no growth of the H4 resonance occurs, but when the methyl protons of the ligand are irradiated, growth of the H4 resonance is observed. This suggests that the ligand has a preferred orientation in space with respect to the cyclopentadienyl ring, such that the *ortho* methyl group lies on the same side of the ring as the proton H4, and the *meta/para* ring protons on the same side of the ring as protons H2 and H5.

Since the interaction of the H2, H4 and H5 protons with L is determined by L, it is tempting to relate this interaction to the size of L. Access to positions near H2 will become limited as the size of L increases, and hence the ratio H2:H4 or H2:H5 should give some measure of the size of L. Thus, the ratio corresponding to the growth of the ring proton resonances in the nOe spectra, H2:H4 (or H5), is predicted to be PMe_3 (118°) > P(O-*o*-tol)$_3$ (141°) > PPh_3 (145°) on steric grounds, as is observed.

2.2.2. NMR analysis: steric measurements

We have devised an experimental procedure using $[(\eta^5\text{-}C_5H_3R_2)M(CO)(L)I]$ complexes to examine the concepts of solid and cone angles. In this approach, multinuclear NMR techniques [3] are used to evaluate the splitting of the various NMR spectral parameters associated with atoms of the cyclopentadienyl ring and its substituents in pseudo-*geminal* arrangements. Correlation of these various spectral parameters with ligand steric parameters (θ, Ω) allows for an evaluation of steric interactions between the cyclopentadienyl ring and L. This approach permits an evaluation of θ and Ω with distance from an apex (the metal). When good correlations are obtained, the implication is that significant steric correlation exists between the ligand and the ring; when poor correlations are observed, little or no steric correlation exists. This type of analysis should give some indication of the cone or solid angle limit; i.e. the distance at which size measurement of the ligand is no longer appropriate using the accepted steric measurements (e.g. θ).

Our previous studies into the analogous $[(\eta^5\text{-}C_5H_3(SiMe_3)_2)Fe(CO)(L)I]$ complexes [3] suggested that steric interaction could be detected as far out from the cyclopentadienyl ring as the carbon atoms of the trimethylsilyl groups, but that the greatest steric interaction was between the silicon atoms and L.

In a similar approach, we have used ^1H and ^{13}C NMR spectroscopy to examine steric interactions between various pseudo-*geminal* arrangements around the stereogenic ruthenium atom and L. A correlation of the type $\Delta = bS + c$, where Δ is the chemical shift separation between the two relevant resonances and S is a measure of steric size, resulted in poor to fair correlations between S and Δ. Since electronic effects are expected to influence the parameters, as found previously [1,3], an electronic parameter was included in the analysis, i.e. $\Delta = aE + bS + c$, where E is an electronic parameter. In this study the electronic parameter chosen was ν_{CO}, while the Tolman cone angle θ [4] and solid angle Ω_s [5] were used as steric parameters for L. The results of these correlations are listed in Table 3. Clearly, the best correlations were obtained between L and the

Table 3
Linear regression data[a] for $\Delta = a(\nu_{CO}) + bS + c$, $S = \theta$, Ω_s

Δ	θ		Ω_s	
	R^2	*mse*	R^2	*mse*
Δ(C4–C5)	0.70	58.34	0.59	79.13
Δ(H4–H5)	0.58	0.45	0.57	0.45
Δ(C6–C7)	0.67	0.040	0.75	0.079
Δ(H6–H7)	0.91	0.0032	0.96	0.018

[a] $R^2 = 1 - \sum_i \frac{\varepsilon_i^2}{(y_i - \bar{y})^2}$, squared multiple correlation coefficient. $mse = \sum_i \varepsilon_i^2$, mean square variance.

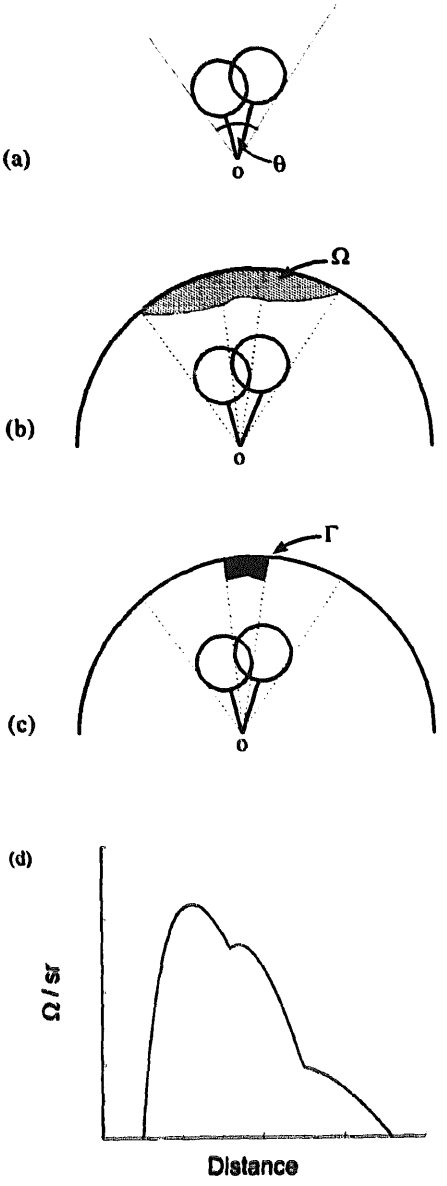

Fig. 6. Illustration of the steric measurements about a point used in this paper. (a) The Tolman cone angle θ [4] is the angle which subtends the two spheres. (b) The area of the projection of the spheres onto a unit sphere is the solid angle Ω of the system [5]. (c) The solid angle of overlap Γ is the projected area of intersection, or overlap, (dark shaded region) of the spheres [6]. (d) Quantification of the variation of the solid angle with distance (e.g. of the two spheres shown in (b)) gives the solid angle radial profile [8].

hydrogen atoms of the trimethylsilyl ring substituents. This is in contrast to the corresponding $[(\eta^5\text{-}C_5H_3(SiMe_3)_2)Fe(CO)(L)I]$ system, where this technique revealed that the best correlation was between L and the carbon atoms of the trimethylsilyl groups.

2.2.3. Analysis of NMR, steric and electronic parameters

While the Tolman cone angle is used as the standard for measuring ligand size in inorganic chemistry (Fig. 6(a)), we and others have attempted to extend the original concept to permit quantification of ligand meshing and size variation with distance from the metal [5]. Our studies have suggested that the use of solid angles to incorporate the above issues have certain advantages.

A consideration of our algorithm for the evaluation of solid angles Ω [5], recently updated [11], has suggested that it can also be used to evaluate possible interactions between adjacent ligands attached to a common origin (e.g. a metal atom). This implies that steric interaction between ligands can, in principle, be quantified. Details of the approach are to be found in previous publications [5–8], but the basic principles are described below.

The solid angle Ω is a representation of ligand size as defined by projection (Fig. 6(b)). While the solid angle is measured at the same position along the ligand as the Tolman cone angle, the shape of the ligand is also considered by this method of size determination. Extension of the methodology to determine the solid angle at variable positions along the ligand generates a solid angle radial profile (SARP) [8].

Two issues relating to SARPs are highlighted in this publication.

1. In the Tolman cone angle, the cone generated from the apex (metal) that encompasses the ligand is assumed to extend to infinity. In reality it hould only extend to the furthest point along the ligand. SARPs can be used to indicate the limit to which the ligand extends away from the apex (metal). It is to be noted that an equivalent measure for cone angles, CARP, has previously been described [8].

2. If two ligands are connected to a common origin (i.e. a metal atom) and are found to occupy the same region in space, then the amount of ligand overlap can be determined by applying the algorithm derived for solid angle measurements; the solid angle of overlap (Γ) at a point can be determined (Fig. 6(c)). The size of the overlap as a function of distance (from the metal), the solid angle of overlap radial profile, can also be evaluated. This region of overlap permits quantification of ligand–ligand overlap with distance from an origin (e.g. a metal atom) [6] (a simpler technique, the vertex angle of overlap (λ), can be used to evaluate steric interactions, but this approach leads to less accurate results; see Ref. [12]).

In this publication we have applied the solid angle of overlap methodology to rationalise the NMR rotational behaviour found in $[(\eta^5\text{-}C_5H_3(SiMe_3)_2)Ru(CO)(L)I]$ (and $[(\eta^5\text{-}C_5H_3(SiMe_3)_2)Fe(CO)(L)I]$) complexes.

2.3. The influence of the metal on intramolecular steric interactions: analysis by radial profiles

It is possible to use both solid angle radial profiles [7] and solid angle of overlap (Γ) radial profiles [6] to interpret the above experimental results. In order to assess the steric interaction between the ligand bonded

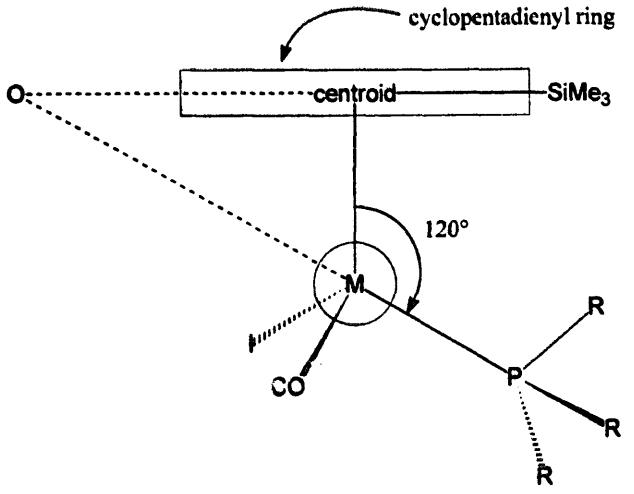

Fig. 7. Side view of $[(\eta^5\text{-}C_5H_3(SiMe_3)_2)M(CO)(PR_3)I]$. Point O corresponds to the origin for measuring the radial profiles of the molecule.

to the metal with the trimethylsilyl substituent of the cyclopentadienyl ring, it is necessary to use the point of intersection of the two vectors shown in Fig. 7 as the origin of the radial profiles. If the metal was used as the origin of the radial profile, the information obtained from the profile would relate to the space occupied by the entire cyclopentadienyl ligand, rather than the substituents on the ligand. The origin chosen places the two groups in the same spatial relationship to allow for direct comparison of steric interactions.

Examination of the CARPs and SARPs (not shown) of the PMe_3 ligand and $SiMe_3$ ring substituent for both the iron and ruthenium complexes reveals that any steric interaction between the groups would probably occur at a greater distance along the ligands in the ruthenium case. However, the difference between the two sets of radial profiles is not very great. It is important to bear in mind that the solid angle radial profile does not quantify

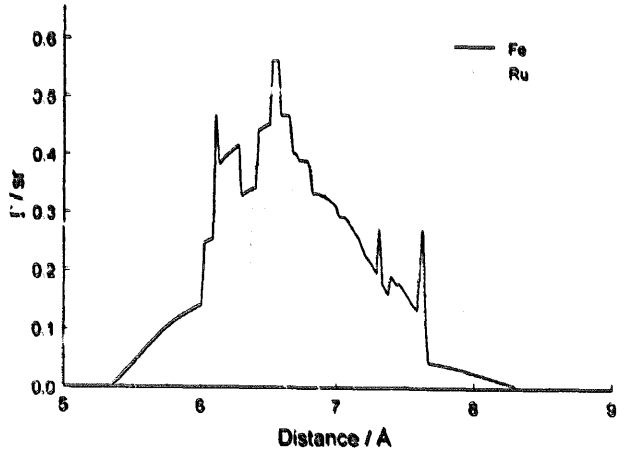

Fig. 8. Solid angle of overlap radial profiles of $[(\eta^5\text{-}C_5H_3(SiMe_3)_2)Fe(CO)(PMe_3)I]$ and $[(\eta^5\text{-}C_5H_3(SiMe_3)_2)Ru(CO)(PMe_3)I]$.

the amount of overlap that will occur; it only quantifies the steric demands of the individual ligands with distance. Thus, the relative proximity of the ligands in space is not accounted for by the solid angle radial profile. The cone angle radial profile has also not been found to be very useful in evaluating steric effects with distance [8].

Of greater interest are the solid angle of overlap profiles of a ligand, e.g. PMe_3, and the $SiMe_3$ ring substituent in the iron and ruthenium systems (Fig. 8). These clearly reveal that, although the type of steric overlap in both systems is similar, significant differences do occur. At distances close to O (the origin for the profile calculations), the ruthenium complex experiences significantly less overlap. Thus, a visual inspection of the solid angle of overlap profiles qualitatively explains why rotation of the cyclopentadienyl ligand in the ruthenium complex, but not the iron complex, is observed. This may also explain the smaller cyclopentadienyl ring proton coupling and ring resonance splitting for the ruthenium system compared with iron. Overall, the ruthenium complex experiences less steric overlap between L and the cyclopentadienyl ligand, and this would further suggest that electronic effects are more important in assessing NMR data for Ru than Fe, as observed.

Although the bonds for ruthenium are longer to both the cyclopentadienyl ring and the PMe_3 ligand than for iron, the ratio of the respective bond lengths for iron and ruthenium is different (Table 4 [13], i.e. cyclopentadienyl centroid Ru:Fe 1.11:1; PMe_3 Ru:Fe 1.03:1). Thus, it is the relatively greater elongation of the metal–cyclopentadienyl ligand bond in the ruthenium complex which allows for a greater degree of rotation than in the corresponding iron complexes.

The strength of this approach is substantiated by the Γ radial profiles for the complexes $[(\eta^5\text{-}C_5H_3(SiMe_3)_2)Ru(CO)(L)I]$, L = ^{t}BuNC, PMe_3, PBz_3 (Fig. 9). It was found that use of the ^{t}BuNC ligand resulted in both single and double substitution of the carbonyl ligands. As can be seen in Fig. 9, only minimal steric overlap occurs between the ^{t}BuNC ligand and the $SiMe_3$ group of the cyclopentadienyl ligand. By contrast, the Γ

Table 4
Distances used in calculating Ω and Γ radial profiles in $[(\eta^5\text{-}C_5H_3(SiMe_3)_2)M(CO)(L)I]$ complexes

Distance	Fe/Å	Ru/Å
Metal–centroid	1.706	1.892
Metal–PMe_3	2.246	2.307
Metal–PBz_3	2.237	2.370
Metal–^{t}BuNC	1.862	1.986
Origin–centroid	2.995	3.277
Origin–metal	3.412	3.784

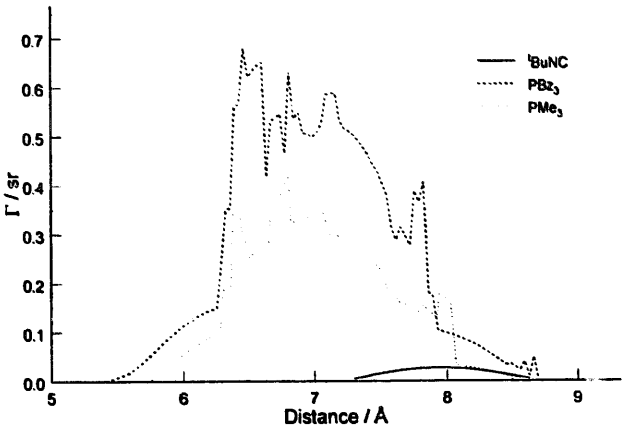

Fig. 9. Solid angle of overlap radial profiles of $[(\eta^5\text{-}C_5H_3(SiMe_3)_2)\text{-}Ru(CO)(L)I]$, L = ^{t}BuNC, PMe_3, PBz_3.

radial profile for the PBz_3 ligand shows greater overlap than the PMe_3 profile, which would suggest that steric factors could explain why no substitution by this large ligand has occurred. Interestingly, in the iron complexes, in which substitution by the PBz_3 ligand did occur, similar Γ radial profiles are found for both the PMe_3 and PBz_3 ligands (not shown).

3. Conclusion

Synthesis of $[(\eta^5\text{-}C_5H_3(SiMe_3)_2)Ru(CO)(L)_2I]$ proved facile in the presence of $[(\eta^5\text{-}C_5H_3\text{-}(SiMe_3)_2)Ru(CO)_2]_2$ catalyst. Both high (no substitution) and low (double substitution) limits were encountered in the carbonyl substitution reaction which relate to steric (and electronic) effects.

Compared with the analogous $[(\eta^5\text{-}C_5H_3(SiMe_3)_2)\text{-}Fe(CO)(L)I]$ complexes, the effect of the larger ruthenium atom on the NMR spectra of the complexes was observed in a number of ways. Firstly, the ruthenium complexes showed complete, although limited, rotation of the cyclopentadienyl ring, as opposed to a 'windscreen wiper' type motion observed for the iron complexes. The larger the ligand in question, the more limited the rotation in the ruthenium complexes. Secondly, the cone angle limit was found to extend further in space for the ruthenium complexes. This impacted on the correlation of NMR parameters with ligand cone or solid angles, and provides an explanation of the lack of Δ(H2–H5) relationship with θ observed for $[(\eta^5\text{-}C_5H_4Me)Ru(CO)(L)I]$ complexes [2]. The difference Δ(H2–H5) was found to be smaller for the ruthenium than for the iron complexes. Solid angle and solid angle of overlap radial profiles proved to be useful tools in accounting for these results by quantifying the positions of steric interaction within the molecule. In particular, solid angle of overlap radial profiles are very useful in accounting for steric properties as both the amount and position of steric overlap can be quantified.

4. Experimental

All phosphine, phosphite and isonitrile ligands were obtained from commercial sources and used without further purification. 1,3-Bis(trimethylsilyl)cyclopentadiene was prepared by a literature procedure [14]. All operations were performed under nitrogen in a well-ventilated fume cupboard, using freshly distilled, dry, deoxygenated solvents. Column chromatography was performed on silica gel using dichloromethane/hexane mixtures as eluent. IR spectra were recorded on a Bruker IFS25 FTIR spectrometer in C_6D_6. NMR spectra were recorded on a Bruker AC-200 spectrometer in C_6D_6. Microanalyses were performed by the Division of Materials Science and Technology, Council for Scientific and Industrial Research, Pretoria.

4.1. Synthesis of $[(\eta^5\text{-}C_5H_3(SiMe_3)_2)Ru(CO)_2I]$

$Ru_3(CO)_{12}$ (395 mg, 0.618 mmol) was added to a two-necked round-bottomed flask containing heptane (100 ml), followed by distilled, pure 1,3-bis(trimethylsilyl)cyclopentadiene. The reaction mixture was heated at reflux for 24 h. Heating of the reaction was stopped and methyl iodide (0.325 ml, 5.22 mmol) was added. The reaction was then allowed to proceed for a further 24 h at room temperature. The solvent was then removed in vacuo and the product purified by column chromatography. The first fraction was found to contain the required product, $[(\eta^5\text{-}C_5H_3(SiMe_3)_2))Ru(CO)_2I]$ (549 mg, 60%) and the second the corresponding dimer, $[(\eta^5\text{-}C_5H_3(SiMe_3)_2)Ru(CO)_2]_2$. Characterisation details are presented in Tables 1 and 2.

4.2. Synthesis of $[(\eta^5\text{-}C_5H_3(SiMe_3)_2)Ru(CO)(L)I]$, L = PMe_3, PPh_2Me, PPh_2Et, PPh_3, $P(OMe)_3$, $P(O^iPr)_3$, $P(OPh)_3$, and $P(O\text{-}o\text{-}tol)_3$

The dicarbonyl complex $[(\eta^5\text{-}C_5H_3(SiMe_3)_2)\text{-}Ru(CO)_2I]$ (ca. 100 mg, 203 μmol) was added to a two-necked round-bottomed flask followed by benzene (50 ml) and the catalyst, $[(\eta^5\text{-}C_5H_3(SiMe_3)_2)\text{-}Ru(CO)_2]_2$. Excess ligand L was added to the mixture, and the reaction heated at reflux. The progress of the reaction was monitored by TLC and by the disappearance of the 2040 cm^{-1} peak in the IR spectrum. On completion of the reaction, the colour of the solution was observed to have changed from brown to red. The solution was cooled, the solvent removed in vacuo and the product purified by column chromatography. All products were isolated as red–brown oils, except for the complexes with L = PMe_3 and PPh_3 which were solids.

Spectroscopic characterisation details are reported in Tables 1 and 2. Analytical details: L = PMe_3, C 33.4% (expected 33.3%), H 5.57% (expected 5.58%); L = PPh_3, C 49.7% (expected 49.5%); H 5.03% (expected 4.85%).

4.3. Synthesis of $[(\eta^5\text{-}C_5H_3(SiMe_3)_2)Ru(CO)_n(^tBuNC)_{2-n}I]$, $n = 0, 1$

A solution of $[(\eta^5\text{-}C_5H_3(SiMe_3)_2)Ru(CO)_2I]$ (84 mg, 170 μmol) and ^{t}BuNC (30 μl, 265 μmol) in benzene (100 ml) was heated to reflux with $[(\eta^5\text{-}C_5H_3(SiMe_3)_2)Ru(CO)_2]_2$ (10 mg). The progress of the reaction was monitored by TLC and IR spectroscopy. On completion of the reaction, the solvent was removed in vacuo to yield a dark oil, which was purified by column chromatography. Two brown oily complexes were isolated, the first identified as $[(\eta^5\text{-}C_5H_3(SiMe_3)_2)Ru(CO)(^tBuNC)I]$ (46 mg, 49%), and the second as $[(\eta^5\text{-}C_5H_3(SiMe_3)_2)Ru(^tBuNC)_2I]$ (35 mg, 34%). Spectroscopic details are reported in Tables 1 and 2.

4.4. Radial profile calculations of $[(\eta^5\text{-}C_5H_3(SiMe_3)_2)M(CO)(L)I]$, M = Fe, Ru; L = PMe_3, PBz_3, ^{t}BuNC

The PMe_3, PBz_3 and $C_5H_3(SiMe_3)_2$ ligand conformations used have been determined previously [5]. The conformation of ^{t}BuNC was obtained from the crystal structure of $[(\eta^5\text{-}C_5H_5)Ru(PPh_3)(^tBuNC)I]$ [15]. For both metal systems, a common origin for the profiles was determined as in Fig. 6. Idealised structures with a centroid–M–L angle of 120° and averaged M–C_5H_5 and M–L bond lengths, as shown in Table 4, were used [13]. Small errors in the angle used have been shown not to have a substantial effect on the final results [16]. The origin for profile calculations was thus at the point of intersection of the vector through the ring centroid and *ipso* carbon with the vector along the metal–phosphorus bond (see Fig. 7). The solid angle radial profiles were calculated by the methodology presented previously [7], using an improved algorithm [11]. Solid angle of overlap profiles were also calculated as by the method previously presented [6], with only non-bonded overlap considered.

Acknowledgements

The authors wish to thank the FRD and the University of the Witwatersrand for providing financial support, and Dr. L. Carlton for recording the nOe spectra.

References

[1] P. Johnston, M.S. Loonat, W.L. Ingham, L. Carlton and N.J. Coville, *Organometallics, 6* (1987) 2121; K.E. du Plooy, C.F. Marais, L. Carlton, R. Hunter, J.C.A. Boeyens and N.J. Coville, *Inorg. Chem., 28* (1989) 3855; N.J. Coville, M.S. Loonat, D. White and L. Carlton, *Organometallics, 11* (1992) 1082.
[2] M.S. Loonat, L. Carlton, J.C.A. Boeyens and N.J. Coville, *J. Chem. Soc., Dalton Trans.*, (1989) 2407.
[3] D. White, L. Carlton and N.J. Coville, *J. Organomet. Chem., 440* (1992) 15.
[4] C.A. Tolman, *Chem. Rev., 77* (1977) 313.
[5] D. White, B.C. Taverner, P.G.L. Leach and N.J. Coville, *J. Comput. Chem., 14* (1993) 1042; D. White and N.J. Coville, *Adv. Organomet. Chem., 36* (1994) 95; D. White, B.C. Taverner, N.J. Coville and P.W. Wade, *J. Organomet. Chem., 495* (1995) 41.
[6] B.C. Taverner, J.M. Smith, D.P. White and N.J. Coville, *S. Afr. J. Chem.*, submitted.
[7] D. White, B.C. Taverner, P.G.L. Leach and N.J. Coville, *J. Organomet. Chem., 478* (1994) 205.
[8] J.M. Smith, B.C. Taverner and N.J. Coville, submitted to *J. Organomet. Chem.*
[9] E. Cesarotti, A. Chiesa, G.F. Ciani, A. Sironi, R. Vefghi and C. White, *J. Chem. Soc., Dalton Trans.*, (1984) 653.
[10] N.J. Coville, Synthetic applications of electron transfer catalysis: the ligand substitution reaction, in W.C. Trogler (ed.), *Organometallic Radical Processes*, Elsevier, Amsterdam, 1990, Chap. 4.
[11] B.C. Taverner, *J. Comput. Chem.*, in press.
[12] J.M. Smith, D.P. White and N.J. Coville, *Polyhedron, 15* (1996) 4541.
[13] A.G. Orpen, L. Brammer, F.H. Allen, O. Kennard, D.G. Watson and R. Taylor, *J. Chem. Soc., Dalton Trans.*, (1989) S1.
[14] J. Okuda, *Top. Curr. Chem., 160* (1991) 1 and references cited therein.
[15] F.M. Conroy-Lewis, A.D. Redhouse and S.J. Simpson, *J. Organomet. Chem., 366* (1989) 357.
[16] D.P. White and N.J. Coville, unpublished results.